Scientific Research

Quantum Chemical Studies of Endofullerenes (M@C$_{60}$) Where M = H$_2$O, Li$^+$, Na$^+$, K$^+$, Be^{2+}, Mg^{2+}, and Ca^{2+}

Osmair Vital de Oliveira, Arlan da Silva Gonçalves*

Department of Chemistry, Instituto Federal do Espírito Santo, Vila Velha, Brazil
Email: osmair@ifes.edu.br, *agoncalves@ifes.edu.br

Abstract

Quantum chemical calculations were performed to investigate the structural and electronic properties of seven endofullerenes. The interaction energies indicated that all of the chemical species are stable inside the fullerene for each complex. The ionization potential and electron affinity values suggest that the endofullerenes consisting of alkaline earth ions are the most reactive and that the dipole moment decreased according to the following order: Be^{2+}@C$_{60}$ (4.75) > Mg^{2+}@C$_{60}$ (3.14) > Ca^{2+}@C$_{60}$ (2.24) > Li$^+$@C$_{60}$ (1.26) > Na$^+$@C$_{60}$ (0.76) > H$_2$O@C$_{60}$ (0.24) > K$^+$@C$_{60}$ (0.00 Debye). These results imply that the solubility of endofullerenes in a polar solvent may increase from H$_2$O@C$_{60}$ to Be^{2+}@C$_{60}$. The energetic gaps indicate that Be^{2+}@C$_{60}$ and Mg^{2+}@C$_{60}$ possess a higher electrical conductivity, and the UV spectra show a shift in the bands to the visible light region. The results of this work may be useful for the development of new endofullerenes.

Keywords

Fullerenes, TDDFT, Electronic Properties, New Materials

1. Introduction

Fullerene (C$_{60}$), which was discovered in 1985 by Kroto *et al*., is the third allotropic form of carbon [1]. The most well-known structure of C$_{60}$ is the Buckminsterfullerene, which consists of 20 hexagonal rings and 12 pentagonal rings that form a geometric structure with 32 faces, which form a closed cage. Each carbon atom is bonded to three others with sp^2 hybridization, and C$_{60}$ tends to react readily with electron rich species due its poor electron delocalization. Since the discovery of C$_{60}$ [1], the literature has reported the development of sev-

---

*Corresponding author.

eral fullerene derivatives based on the functionalization of the C_{60} cage aiming to produce new properties and/or improve their existing properties. Other important studies involve the use of C_{60} derivatives in biological systems [2]-[4], solar cells [5]-[8] and superconductors [9]-[11]. Another class of C_{60} derivatives has been achieved by the encapsulation of small molecules, metals and ions inside the C_{60} cage. This type of system is known as an endofullerene (nomenclature proposed by Chai *et al.*) [12]. This representation is referred to as $A@C_n$, where A and n are the chemical species and the number of carbon atoms, respectively. Among the endofullerenes, those based on C_{60} have attracted much attention due their potential applications in superconductivity and materials science [13]-[15]. The first evidence of metal trapped inside C_{60} was obtained by Heath and collaborators [16], who reported the formation of the $La@C_{60}$ complex. In the same laboratory, an air-stable film of $La@C_{60}$ was obtained [12]. $Li^+@C_{60}$ was the first endohedral to be isolated, characterized and its crystal structure elucidated [17] [18]. Other non-metal C_{60} endofullerenes have been experimentally determined including $H_2@C_{60}$ [19] [20], $N_2@C_{60}$ [21], noble gas [22] [23], and, more recently, $H_2O@C_{60}$ [24]-[26].

C_{60} endofullerenes can be obtained using three different experimental methods [27] including 1) the vaporization of graphite, 2) the insertion of the atoms through the fullerene cages, and 3) chemical routes that involve opening the fullerene cage. However, this method involves the use of extreme conditions, such as high temperature and treatment with high pressure. The increased energy expenditure results in endofullerene synthesis having high costs. Theoretical methods based on quantum chemistry are useful for predicting important properties that, in general, confirm the experimental data. Several theoretical studies of C_{60} endofullerenes have been reported. Among these studies, quantum chemistry has been employed to study 1) the structural and optical properties of endofullerenes [28], 2) the mechanism of alkali-metal insertion into C_{60} [29], 3) electronic structures [30] [31], 4) the charge transfer from the metal to C_{60} [32] [33], 5) the insertion of Be into C_{60} [34], and 6) the photoionization cross section in $Mg^{2+}@C_{60}$ [35]. Although some alkali and alkaline earth ions have been studied using quantum chemical methods [28]-[35], the reactivity parameters of the current endofullerenes have not been predicted. However, some properties are very important in the chemical synthesis. Therefore, the goal of the current work was to investigate the electronic and structural properties of $M@C_{60}$ (where M = H_2O, Li^+, Na^+, K^+, Be^{2+}, Mg^{2+}, and Ca^{2+}) using quantum chemical methods. We have considered $H_2O@C_{60}$ and pure C_{60} to be reference systems when comparing the properties of a non-metallic endofullerene with the metallic ions complexes. Here, we are interested in predicting the reactivity parameters, electrical conductivity, absorption spectra, polarization and charge transfer process.

2. Computational Details

The C_{60} structure was retrieved from the Library of 3-D Molecular Structures [http://www.nyu.edu/pages/mathmol/library/]. The endofullerenes were initially constructed by inserting the chemical species into the center of the fullerene using PyMOL [http://www.pymol.org/]. In sequential calculations, all of the structures were initially optimized using semi-empirical PM7 Hamiltonian [36], as implemented in the MOPAC package [37]. The final structures from these calculations were re-optimized using the GAMESS-US software [38] using DFT/B3LYP hybrid functional [39] [40] with the 6-31G(2d,2p) basis set. All of the stationary points were characterized as a point of minimum energy using the harmonic vibrational and ZPE correction calculations with the 6-31G(2d,2p) basis set. The absorption spectra were calculated using the TDDFT method with the 6-31G basis set, as implemented in the GAMESS-US software [38]. This basis set was used to reduce the high computational cost of the TDDFT calculations, and the polarizable continuum model (PCM) [41] of solvation was employed to account for the solvent (toluene) effects.

3. Results and Discussion

At the end of the optimizations, which were conducted using different methodologies, the spatial structures were aligned, and the RMSD (root mean square deviation) was calculated based on the DFT optimized structure, which was used as a reference. Surprisingly, the RMSD values were lower than 0.001 Å for all of the endofullerenes except $Be^{2+}@C_{60}$ and $Mg^{2+}@C_{60}$, for which the RMSD was 0.01 Å. These small values indicate that the endofullerene structures obtained using the semi-empirical PM7 and DFT methods are very similar. Therefore, these methods possessed similar accuracies for the prediction of the current endofullerene structures. However, all of the reported results have been extracted from the DFT optimized structures (**Figure 1**).

The results in **Figure 1** indicate that in all of the endofullerenes except $H_2O@C_{60}$ and $K^+@C_{60}$, the ions are
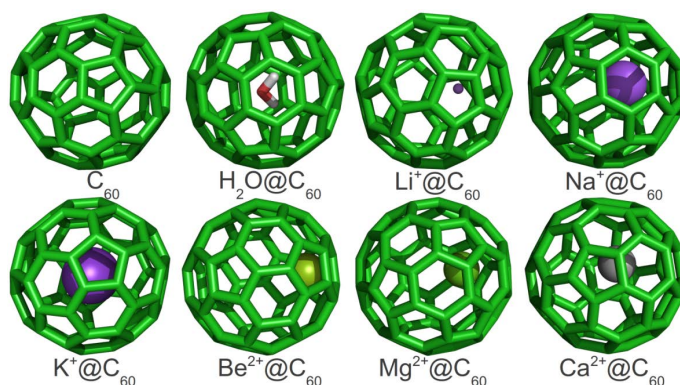
Figure 1. DFT/B3LYP/6-31G** optimized structures. The ion size is proportional to the van der Waals radius. The carbon atoms are shown in green.

located in an off-center position in the C_{60}. In addition, these ions are near the six-membered ring, with a distance of 2.3, 2.8, 1.8 and 2.6 Å for Li^+, Na^+, Be^{2+} and Ca^{2+} ions, respectively. The Li^+...C distance in the crystallographic structure (2.3 Å) [17] and our optimized molecule are the same, which demonstrates the accuracy of the current theoretical protocols. In $K^+@C_{60}$, the K^+ ion is located in the center of the C_{60} cage, which is in agreement with the results from previous calculations [42]. This behavior can be attributed to the high ionic size of K^+ compared with the other studied ions. For the optimized $H_2O@C_{60}$ complex, the shortest H...C and O...C distances are 2.70 and 3.45 Å, respectively, which is consistent with the crystallographic structure [26], where the H...C and O...C interatomic distances are 2.60 and 3.55 Å, respectively. In addition, we performed an optimization with a single water molecule using the same theoretical level to compare the various properties obtained with the water molecule encapsulated in C_{60}. In this calculation, the H-O bonds had the same distance (0.96 Å). However, the H-O-H angle was different (*i.e.*, $H_2O@C_{60}$ = 103.72° and pure water = 104.13°). A decrease of 0.4% in this angle was most likely due to electronic repulsion between the hydrogen and carbon atoms. The endofullerene stability was based on the total energy (in hartree) obtained by DFT optimizations. The stability of the endofullerenes increased in the following order: C_{60} (−2284.8) > $Li^+@C_{60}$ (−2292.2) > $Be^{2+}@C_{60}$ (−2298.9) > $H_2O@C_{60}$ (−2361.2) > $Na^+@C_{60}$ (−2446.9) > $Mg^{2+}@C_{60}$ (−2484.2) > $K^+@C_{60}$ (−2884.5) > $Ca^{2+}@C_{60}$ (−2961.8).

In all of the optimized structures, the encapsulation of the chemical species is favorable (negative values of ΔE). **Table 1** summarizes some of the electronic properties obtained from the calculations.

According to Koopmans' theorem, the ionization potential (IP) of a molecule is the highest orbital molecular orbital (HOMO) energy (ε_{HOMO}) multiplied by −1, and the lowest unoccupied molecular orbital (LUMO) energy (ε_{LUMO}) multiplied by −1 represents the electron affinity (EA) or the capacity of a molecule to accept electrons. In a simplistic reaction model, the LUMO would be expected to accept electrons from the HOMO of another molecule. The results in **Table 1** indicate that the endofullerenes containing ions in the same family have a similar IP, with values of ~9.20 and ~12.36 eV for alkali and alkaline earth ions, respectively. Therefore, the size of ionic radius and the IP of the ions in the same family do not effectively contribute to the IP of C_{60} endofullerenes. However, the IP of endofullerenes increases by ~31% when alkali ions are replaced by alkaline earth ions. This increase is due to the high IP values of the alkaline earth ions compared with the alkali ions. Interestingly, the presence of the water molecule in the C_{60} decreased its IP, which indicated that the C_{60} endofullerene is more electron donor than the pure C_{60}. In contrast, an increase in the IP was observed for the metal endofullerenes because they are more electron acceptor than C_{60}. Therefore, in both cases, the ions transfer their ionic character to C_{60} in the encapsulation process. The same behavior was observed for the electron affinity (LUMO orbital energy), as shown in **Table 1**. The EA is more negative for all of the C_{60} endofullerenes studied than it is for pure C_{60}, which indicated that the endofullerenes are more electron accepting compared with pure fullerene. Other chemical properties that can be estimated from the ε_{LUMO} and ε_{HOMO} include the chemical potential, μ ((ε_{LUMO} + ε_{HOMO})/2), and the chemical hardness, η((ε_{LUMO} − ε_{HOMO})/2). μ and η measure the tendency of an electron to escape from a particular field [43] and the resistance to modification of the electronic density [44], respectively. Therefore, the low values of μ and η for the alkaline earth ion C_{60} endofullerenes indicated that these

Table 1. Properties obtained from quantum chemical calculations at the DFT/B3LYP/6-31G** level.

M@C_{60}	ΔE^a	ε_{HOMO}/eV	ε_{LUMO}/eV	μ/eV	η/eV	Dipole/D	M charges[b]
C_{60}	0.00	−5.93	−3.03	−4.48	1.45	0.00	---
H_2O@C_{60}	−0.09	−5.87	−3.14	−4.50	1.37	0.34	0.19
Li@C_{60}	−1.01	−9.17	−6.51	−7.84	1.33	1.26	0.58
Na@C_{60}	−0.89	−9.22	−6.47	−7.84	1.38	0.76	0.58
K@C_{60}	−0.65	−9.22	−6.45	−7.84	1.39	0.00	0.62
Be@C_{60}	−11.96	−12.32	−10.34	−11.33	0.99	4.75	0.36
Mg@C_{60}	−5.20	−12.35	−10.96	−11.66	0.70	3.14	0.53
Ca@C_{60}	−5.15	−12.43	−9.90	−11.17	1.27	2.24	0.72

[a] $\Delta E = E_{M@C_{60}} - \left(E_M + E_{C_{60}}\right)$ in kcal/mol; [b]ChelpG charge of encapsulated chemical species.

complexes are more resistant to donating an electron and that their electronic density is more easily modified compared with the other endofullerenes. In other words, the endofullerenes based on alkaline earth ions are more reactive than are the other endofullerenes studied. Among the M@C_{60} complexes, Mg^{2+}@C_{60} exhibited the lowest values of μ (−11.66 eV) and η (0.70 eV), which is expected to result in high reactivity. The degree of fullerene polarization was characterized by the dipole moment. Except for K^+@C_{60}, all of the studied chemical species increased the C_{60} polarizability, and the dipole moment values increased with the decreasing binding energies (ΔE) (**Table 1**). The K^+ ion did not increase the dipole of C_{60} due to the large distance between the carbon atoms and this ion. The dipole moment for H_2O@C_{60} was 0.34 D. Therefore, the water molecule transferred its partial dipole to C_{60}. The calculated dipole moment for pure water obtained using the same theoretical level as that employed for all of the endofullerenes was 2.04 D. By comparing the dipole moment of pure H_2O and H_2O@C_{60}, a decrease of 83% was observed, which is in agreement with the *ab initio* results reported by Shameema [45]. However, Kurotobi and Murata [24] predicted an increase in the dipole moment of 0.05% in H_2O@C_{60} relative to pure water using the MX06-2X functional. This discrepancy may be due to the different functionals used. The dipole moment of the endofullerenes decreased in the following order: Be^{2+}@C_{60} (4.75 D) > Mg^{2+}@C_{60} (3.14 D) > Ca^{2+}@C_{60} (2.24 D) > Li^+@C_{60} (1.26 D) > Na^+@C_{60} (0.76 D) > H_2O@C_{60} (0.24 D) > K^+@C_{60} (0.00 D). This sequence indicates that the solubility of endofullerene in water or other polar solvents may increase from H_2O@C_{60} to Be^{2+}@C_{60}. Therefore, the presence of these chemical species, except for K^+, in the C_{60} cage can improve its solubility. The dipole moment observed for these fullerenes was due to the charge transfer from the chemical species to the fullerene (**Table 1**). Except for water, all of the chemical species positively increased the fullerene charge. For single water, the ChelpG charge of the O and H atoms were −0.72 and 0.36, respectively. In H_2O@C_{60}, the charge of the oxygen increased to −0.46, and the charge of the hydrogen atoms decreased to 0.33 and 0.32. Therefore, a portion of the water charge was transferable to C_{60}, which resulted in a negative charge of −0.19 (**Table 1**). For all of the systems, the carbon atoms nearest the ions acquired a negative charge, while the positive charge was distributed over the C_{60} surface that was far from the metal ions. In general, the charge transfer from the cation to C_{60} increased as the binding energy decreased due to cation-pi electronic interactions. Therefore, Be^{2+} transferred 82% of its charge to the fullerene, and this endofullerene possessed the lowest binding energy (−11.96 kcal/mol).

Electronic conductivity is another interesting and important property of the new materials. This property can be estimated from the difference between the calculated HOMO and LUMO energies using Equation (1).

$$\sigma \propto e^{\frac{-E_g}{2k_bT}} \tag{1}$$

where σ is the electric conductivity, E_g is the band gap energy, k_b is Boltzmann's constant and T is the temperature. This equation indicates that a higher electric conductivity is due to a decrease in E_g. **Figure 2** shows the HOMO and LUMO energies and their surface representations obtained from DFT calculations.

C_{60} acts as a semiconductor with an experimental band gap of 2.3 - 2.7 eV [46]-[49]. Therefore, the value (2.90 eV) that we obtained using the approximation |HOMO − LUMO| (**Figure 2**) is close to the experimental

data. It is interesting to note that for all of the endofullerenes, the calculated energy gap is less than that of pure C_{60}. Based on Equation (1) and the low band gap energy of $Be^{2+}@C_{60}$ (1.98 eV) and $Mg^{2+}@C_{60}$ (1.38 eV), we suggest that these endofullerenes are more conductive than C_{60} and the other studied endofullerenes.

Another important property in the development of new materials is the capacity of a material to absorb in the visible region. **Figure 3** shows the UV spectra of all of the studied compounds.
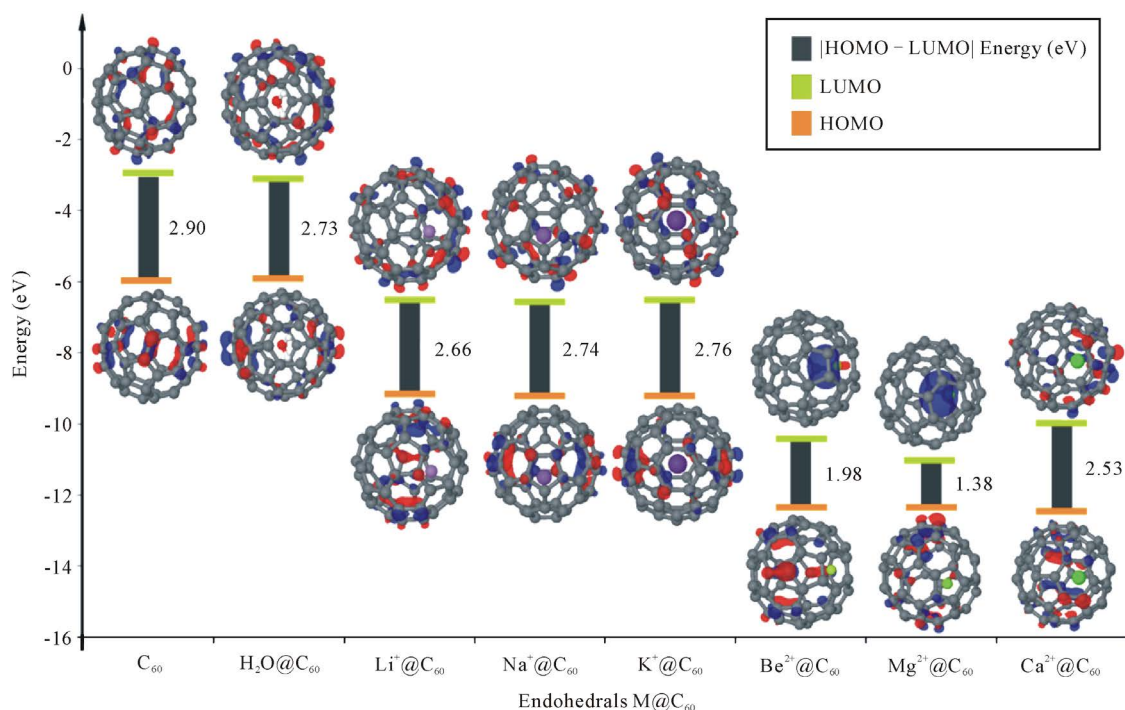

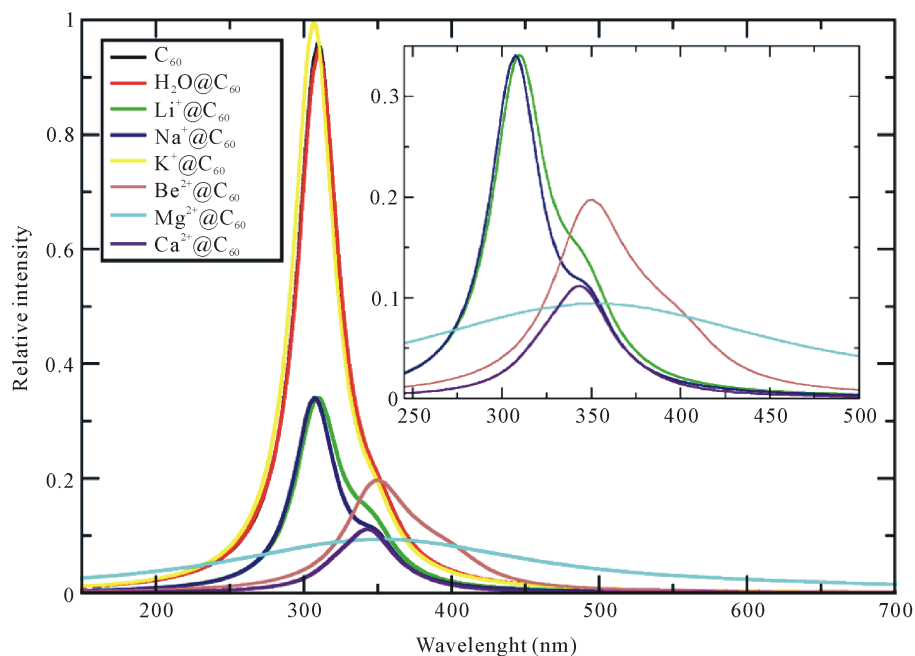**Figure 2.** HOMO and LUMO orbital energies obtained at the B3LYP/6-31G(2d,2p) level.

Figure 3. UV spectra obtained at the B3LYP/6-31G level. Inset shows the zoom of the region (250 - 500 nm, 0 - 0.38).

According to Prylutskyy [50], fullerene in toluene solvent possesses two intense broad absorption bands (*i.e.*, 269 and 335 nm) and allowed transitions. In the current work, the band of major interest is near the UV-visible region (335 nm) because we believe that the presence of ions in C_{60} can shift this band to the visible region. In our calculations, we observed a band centered at 310 nm for a single C_{60}. Because our calculations were performed using PCM [41] with average basis sets, the calculated UV spectra are in reasonable agreement with the experimental data. However, the band at 310 nm for pure C_{60} is in agreement with previous theoretical calculations [51] [52]. In **Figure 3**, the absorption and band intensity of $H_2O@C_{60}$ and $K^+@C_{60}$ are similar to those of pure C_{60}, which is due to the low interaction energy between these species and C_{60} (**Table 1**). For $Li^+@C_{60}$ and $Na^+@C_{60}$, the same wavelength (308 nm) with a relative intensity of 0.34 and a small shoulder at 343 nm was also observed. Interestingly, two bands at 343 (small shoulder) and 350 nm (large shoulder) were observed for $Ca^{2+}@C_{60}$ and $Be^{2+}@C_{60}$, respectively. However, the largest shoulder with a band centered at 356 nm with the lowest relative intensity (0.09) was observed for $Mg^{2+}@C_{60}$. This result reinforces the hypothesis that the presence of Mg^{2+} in C_{60} can shift the absorption spectra to the visible region (**Figure 3**).

4. Conclusion

Chemical species trapped in fullerenes comprise a new class of molecules with interesting properties. Therefore, in the current work, we employed quantum chemical methods to study seven endofullerenes (*i.e.*, $H_2O@C_{60}$, $Li^+@C_{60}$, $Na^+@C_{60}$, $K^+@C_{60}$, $Be^{2+}@C_{60}$, $Mg^{2+}@C_{60}$ and $Ca^{2+}@C_{60}$). Our results indicate that all of the endofullerenes are more stable than pure C_{60}. The total energy (in hartree) calculated using DFT optimizations is as follows: C_{60} (−2284.8) > $Li^+@C_{60}$ (−2292.2) > $Be^{2+}@C_{60}$ (−2298.9) > $H_2O@C_{60}$ (−2361.2) > $Na^+@C_{60}$ (−2446.9) > $Mg^{2+}@C_{60}$ (−2484.2) > $K^+@C_{60}$ (−2884.5) > $Ca^{2+}@C_{60}$ (−2961.8). The reactivity parameters (*i.e.*, ionization potential and electron affinity) indicate that the alkali earth ions trapped in C_{60} are the most reactive. In our calculations, charge transfer was observed from the ions to the fullerene. Therefore, except for $K^+@C_{60}$, the dipole moment increased in the following order: $Be^{2+}@C_{60}$ (4.75 Debye) > $Mg^{2+}@C_{60}$ (3.14 D) > $Ca^{2+}@C_{60}$ (2.24 D) > $Li^+@C_{60}$ (1.26 D) > $Na^+@C_{60}$ (0.76 D) > $H_2O@C_{60}$ (0.24 D) > $K^+@C_{60}$ (0.00 D). Therefore, the solubility of the endofullerenes in polar solvents is expected to follow the same trend. Based on the HOMO and LUMO energy difference, $Be^{2+}@C_{60}$ and $Mg^{2+}@C_{60}$ have the highest electrical conductivity with band gap energies of 1.98 and 1.38 eV, respectively. The UV spectra obtained is in reasonable agreement with the experimental data. The C_{60} band centered at 310 nm shifted to 343, 350 and 356 nm for $Ca^{2+}@C_{60}$, $Be^{2+}@C_{60}$ and $Mg^{2+}@C_{60}$, respectively, which confirms the previous theoretical results.

Acknowledgements

References

[1] Kroto, H.W., Heath, J.R., O'Brien, S.C., Curl, R.F. and Smalley, R.E. (2003) C_{60}: Buckminsterfullerene. *Nature*, **318**, 162-163. http://dx.doi.org/10.1038/318162a0

[2] Bosi, S., Ros, T.D., Spalluto, G. and Prato, M. (2003) Fullerene Derivatives: An Attractive Tool for Biological Applications. *European Journal of Medicinal Chemistry*, **38**, 913-923. http://dx.doi.org/10.1016/j.ejmech.2003.09.005

[3] Bakry, R., Vallant, R.M., Najam-ul-Haq, M., Rainer, M., Szabo, Z., Huck, C.W. and Bonn, G.K. (2007) Medicinal Applications of Fullerenes. *International Journal of Nanomedicine*, **2**, 639-649.

[4] Anilkumar, P., Lu, F., Cao, L., Luo, P.G., Liu, J.H., Sahu, S., Tackett, K.N., Wang, Y. and Sun, Y.P. (2011) Fullerenes for Applications in Biology and Medicine. *Current Medicinal Chemistry*, **18**, 2045-2059. http://dx.doi.org/10.2174/092986711795656225

[5] Blom, P.W.M., Mihailetchi, V.D., Koster, L.J.A. and Markov, D.E. (2007) Device Physics of Polymer: Fullerene Bulk Heterojunction Solar Cells. *Advanced Materials*, **19**, 1551-1566. http://dx.doi.org/10.1002/adma.200601093

[6] Deibel, C. and Dyakonov, V. (2010) Polymer-Fullerene Bulk Heterojunction Solar Cells. *Reports on Progress in Physics*, **73**, Article ID: 096401. http://dx.doi.org/10.1088/0034-4885/73/9/096401

[7] Varotto, A., Treat, N.D., Jo, J., Shuttle, C.G., Batara, N.A., Brunetti, F.G., Seo, J.H., Chabinyc, M.L., Hawker, C.J., Heeger, A.J. and Wudl, F. (2011) 1,4-Fullerene Derivatives: Tuning the Properties of the Electron Transporting Layer in Bulk-Heterojunction Solar Cells. *Angewandte Chemie*, **50**, 5166-5169.

[8] Liu, B., Png, R.Q., Zhao, L.H., Chua, L.L., Friend, R.H. and Ho, P.K. (2012) High Internal Quantum Efficiency in Fullerene Solar Cells Based on Crosslinked Polymer Donor Networks. *Nature Communications*, **3**, 1321. http://dx.doi.org/10.1038/ncomms2211

[9] Tanigaki, K., Ebbesen, T.W., Saito, S., Mizuki, J., Tsai, J.S., Kubo, Y. and Kuroshima, S. (1991) Superconductivity at 33 K in CsxRbyC$_{60}$. *Nature*, **352**, 222. http://dx.doi.org/10.1038/352222a0

[10] Buntar, V. and Weber, H.W. (1996) Magnetic Properties of Fullerene Superconductors. *Superconductor Science and Technology*, **9**, 599-615. http://dx.doi.org/10.1088/0953-2048/9/8/001

[11] Hott, R., Kleiner, R., Wolf, T. and Zwicknagl, G. (2013) Review on Superconducting Materials. Wiley-VCH, Hoboken.

[12] Chai, Y., Guo, T., Jin, C.M., Haufler, R.E., Chibante, L.P.F., Fure, J., Wang, L.H., Alford, J.M. and Smalley, R.E. (1991) Fullerenes with Metals Inside. *Journal of Physical Chemistry*, **95**, 7564-7568. http://dx.doi.org/10.1021/j100173a002

[13] Bethune, D.S., Johnson, R.D., Salem, J.R., Vries, M.S. and Yannoni, C.S. (1993) Atoms in Carbon Cages: The Structure and Properties of Endohedral Fullerenes. *Nature*, **366**, 123-128. http://dx.doi.org/10.1038/366123a0

[14] Hirata, T., Hatakeyama, R., Mieno, T. and Sato, N. (1996) Production and Control of K-C$_{60}$ Plasma for Material Processing. *Journal of Vacuum Science & Technology A*, **14**, 615-619. http://dx.doi.org/10.1116/1.580154

[15] Chaur, M.N., Melin, F., Ortiz, A.L. and Echegoyen, L. (2009) Chemical, Electrochemical, and Structural Properties of Endohedral Metallofullerenes. *Angewandte Chemie International Edition*, **48**, 7514-7538. http://dx.doi.org/10.1002/anie.200901746

[16] Heath, J.R., O'Brien, S.C., Zhang, Q., Liu, Y., Curl, R.F., Tittel, F.K. and Smalley, R.E. (1985) Lanthanum Complexes of Spheroidal Carbon Shells. *Journal of the American Chemical Society*, **107**, 7779-7780. http://dx.doi.org/10.1021/ja00311a102

[17] Aoyagi, S., Nishibori, E., Sawa, H., Sugimoto, K., Takata, M., Miyata, Y., Kitaura, R., Shinohara, H., Okada, H., Sakai, T., *et al.* (2010) A Layered Ionic Crystals of Polar Li@C$_{60}$ Superatoms. *Nature Chemistry*, **2**, 678-683. http://dx.doi.org/10.1038/nchem.698

[18] Okada, H., Komuro, T., Sakai, T., Matsuo, Y., Ono, Y., Omote, K., Yokoo, K., Kawachi, K., Kasama, Y., Ono, S., *et al.* (2012) Preparation of Endohedral Fullerene Containing Lithium (Li@C$_{60}$) and Isolation as Pure Hexafluorophosphate Salt ([Li+@C$_{60}$][PF6-]). *RSC Advances*, **2**, 10624-10631. http://dx.doi.org/10.1039/c2ra21244g

[19] Murata, Y., Murata, M. and Komatsu, K. (2003) 100% Encapsulation of a Hydrogen Molecule into an Open-Cage Fullerene Derivative and Gas-Phase Generation of H$_2$@C$_{60}$. *Journal of the American Chemical Society*, **125**, 7152-7153. http://dx.doi.org/10.1021/ja0354162

[20] Komatsu, K., Murata, M. and Murata, Y. (2005) Encapsulation of Molecular Hydrogen in Fullerene C$_{60}$ by Organic Synthesis. *Science*, **307**, 238-240. http://dx.doi.org/10.1126/science.1106185

[21] Ito, S., Shimotani, H., Takagi, H. and Dragoe, N. (2008) On the Synthesis Conditions of N and N$_2$ Endohedral Fullerenes. *Fullerenes*, *Nanotubes and Carbon Nanostructures*, **16**, 206-213.

[22] Sauders, M., Cross, R.J., Jimenez-Vazquez, H.A., Shimshi, R. and Khong, A. (1996) Noble Gas Atoms inside Fullerences. *Science*, **271**, 1693-1697. http://dx.doi.org/10.1126/science.271.5256.1693

[23] Peng, R.F., Chu, S.J., Hyang, Y.M., Yu, H.J., Wang, T.S., Jin, B., Fu, Y.B. and Wang, C.R. (2009) Preparation of He@C$_{60}$ and He$_2$@C$_{60}$ by an Explosive Method. *Journal of Materials Chemistry*, **19**, 3602-3605. http://dx.doi.org/10.1039/b904234b

[24] Kurotobi, K. and Murata, Y. (2011) A Single Molecule of Water Encapsulated in Fullerene C$_{60}$. *Science*, **333**, 613-616.

[25] Beduz, C., Carravetta, M., Chen, J.C., Consistrè, M., Denning, M., Frunzi, M., *et al.* (2012) Quantum Rotation of Ortho and Para-Water Encapsulated in a Fullerene Cage. *Proceedings of the National Academy of Sciences of the United States of America*, **109**, 12894-12898. http://dx.doi.org/10.1073/pnas.1210790109

[26] Aoyagi, S., Hoshino, N., Akutagawa, T., Sado, Y., Kitaura, R., Shinohrara, H., Sugimoto, K., Zhang, R. and Murata, Y. (2014) A Cubic Dipole Lattice of Water Molecules Trapped inside Carbon Cages. *Chemical Communications*, **50**, 524-526. http://dx.doi.org/10.1039/c3cc46683c

[27] Popov, A.A., Yang, S. and Dunsch, L. (2013) Endohedral Fullerenes. *Chemical Reviews*, **113**, 5989-6113. http://dx.doi.org/10.1021/cr300297r

[28] Noguchi, Y., Sugino, O., Okada, H. and Matsuo, Y. (2013) First-Principles Investigation on Structural and Optical Properties of M$^+$@C$_{60}$ (Where M = H, Li, Na, and K). *Journal of Physical Chemistry C*, **117**, 15362-15368. http://dx.doi.org/10.1021/jp4041259

[29] Malani, H. and Zhang, D. (2013) Theoretical Insight for the Metal Insertion Pathway of Endohedral Alkali Metal Fullerenes. *Journal of Physical Chemistry A*, **117**, 3521-3528. http://dx.doi.org/10.1021/jp4007697

[30] Cioslowski, J. (1991) Endohedral Chemistry: Electronic Structures of Molecules Trapped inside the C_{60} Cage. *Journal of the American Chemical Society*, **113**, 4139-4141. http://dx.doi.org/10.1021/ja00011a013

[31] Cioslowski, J. and Fleischmann, E.D. (1991) Endohedral Complexes: Atoms and Ions inside the C_{60} Cage. *Journal of Chemical Physics*, **94**, 3730-3734. http://dx.doi.org/10.1063/1.459744

[32] Hira, A.S. and Ray, A.K. (1995) Interaction Sites of a Na^+ Ion and a Na Atom with a C_{60} Molecule. *Physical Review A*, **52**, 141-148. http://dx.doi.org/10.1103/PhysRevA.52.141

[33] Santos, J.D., Longo, E., Banja, M.E., Espinoza, V.A.A., Flores, J.V. and Taft, C.A. (2005) Semi-Empirical Studies of Alkaline Metals-Fullerene MxC_{60}, $M@C_{60}$ Interactions. *Journal of Molecular Structure*: *THEOCHEM*, **713**, 161-169. http://dx.doi.org/10.1016/j.theochem.2004.08.055

[34] Ohtsuki, T., Masumoto, K., Ohno, K., Maruyma, Y., Kawazoe, Y., Sueki, K. and Kikuchi, K. (1996) Insertion of Be Atoms in C_{60} Fullerene Cages: $Be@C_{60}$. *Physical Review Letters*, **77**, 3522-3524. http://dx.doi.org/10.1103/PhysRevLett.77.3522

[35] Lyras, A. and Bachau, H. (2005) Electronic Correlation Effects in a Model of Endohedral Mg ($Mg@C_{60}$). *Journal of Physics B*: *Atomic*, *Molecular and Optical Physics*, **38**, 1119-1131. http://dx.doi.org/10.1088/0953-4075/38/8/004

[36] Stewart, J.J.P. (2013) Optimization of Parameters for Semiempirical Methods VI: More Modifications to the NDDO Approximations and Re-Optimization of Parameters. *Journal of Molecular Modeling*, **19**, 1-32. http://dx.doi.org/10.1007/s00894-012-1667-x

[37] Stewart, J.J.P. (2012) MOPAC2012, Stewart Computational Chemistry. Colorado Springs, CO. HTTP://OpenMOPAC.net

[38] Schmidt, M.W., Baldridge, K.K., Boatz, J.A., Elbert, S.T., Gordon, M.S., Jensen, J.H., Koseki, S., Matsunaga, N., Nguyen, K.A., Su, S., Windus, T.L., Dupuis, M. and Montgomery, J.A. (1993) General Atomic and Molecular Electronic Structure System. *Journal of Computational Chemistry*, **14**, 1347-1363. http://dx.doi.org/10.1002/jcc.540141112

[39] Lee, C., Yang, W. and Parr, R.G. (1998) Development of the Colle-Salvetti Correlation-Energy Formula into a Functional of the Electron Density. *Physical Review B*, **37**, 785-789. http://dx.doi.org/10.1103/PhysRevB.37.785

[40] Becke, A.D. (1993) Density Functional Thermochemistry. III. The Role of Exact Exchange. *Journal of Chemical Physics*, **98**, 5648-5652. http://dx.doi.org/10.1063/1.464913

[41] Tomasi, J., Mennucci, B. and Cammi, R. (2005) Quantum Mechanical Continuum Solvation Models. *Chemical Reviews*, **105**, 2999-3094. http://dx.doi.org/10.1021/cr9904009

[42] Dunlap, B.I., Ballester, J.L. and Schmidt, P.P. (1992) Interactions between Fullerene C_{60} and Endohedral Alkali Atoms. *Journal of Physical Chemistry*, **96**, 9781-9787. http://dx.doi.org/10.1021/j100203a038

[43] Parr, R.G., Donnelly, R.A., Levy, M. and Palke, W.E. (1978) Electronegativity: The Density Functional Viewpoint. *Journal of Chemical Physics*, **68**, 3801-3807. http://dx.doi.org/10.1063/1.436185

[44] Parr, R.G. and Pearson, R.G. (1983) Absolute Hardness: Companion Parameter to Absolute Electronegativity. *Journal of the American Chemical Society*, **105**, 7512-7516. http://dx.doi.org/10.1021/ja00364a005

[45] Shameema, O., Ramachandran, C.N. and Sathyamurthy, N. (2006) Blue Shift in X-H Stretching Frequency of Molecules Due to Confinement. *Journal of Physical Chemistry A*, **110**, 2-4. http://dx.doi.org/10.1021/jp056027s

[46] Benning, P.J., Martins, J.L., Weaver, J.H., Chibante, L.P.F. and Smalley, R.E. (1991) Electronic Structure of KxC_{60}: Insulating, Metallic, and Superconducting Character. *Science*, **252**, 1417-1419. http://dx.doi.org/10.1126/science.252.5011.1417

[47] Takahashi, T., Susuzi, S., Morikawa, T., Katayama-Yoshida, H., Hasegawa, S., Inokuchi, H., Seki, K., Kikuchi, K., Suzuki, S., Ikemoto, K. and Ashiba, Y. (1992) Pseudo-Gap at the Fermi Level in K_3C_{60} Observed by Photoemission and Inverse Photoemission. *Physical Review Letters*, **68**, 1232. http://dx.doi.org/10.1103/PhysRevLett.68.1232

[48] Lof, R.W., van Veendaal, M.A., Koopmans, B., Jonkman, H.T. and Sawatzky, G.A. (1992) Band Gap, Excitons, and Coulomb Interaction in Solid C_{60}. *Physical Review Letters*, **68**, 3924. http://dx.doi.org/10.1103/PhysRevLett.68.3924

[49] Weaver, J.H. (1992) Electronic Structures of C_{60}, C_{70} and the Fullerides: Photoemission and Inverse Photoemission Studies. *Journal of Physics and Chemistry of Solids*, **53**, 1433-1447. http://dx.doi.org/10.1016/0022-3697(92)90237-8

[50] Prylutskyy, Y.I., Durov, S.S., Bulavin, L.A., Adamenko, I., Moroz, K.O., Graja, A., Bogucki, A. and Scharff, P. (2001) C 1s Ionisation Potential and Energy Referencing for Solid C_{60} Films on Metal Surfaces. *Fullerene Science and Technology*, **9**, 167-174. http://dx.doi.org/10.1081/FST-100102964

[51] Braga, M., Larsson, S., Rosen, A. and Volosov, A. (1991) Electronic Transition in C_{60}. On the Origin of the Strong Interstellar Absorption at 217nm. *Astronomy and Astrophysics*, **245**, 232-238.

[52] Orlandi, G. and Negri, F. (2002) Electronic States and Transitions in C_{60} and C_{70} Fullerenes. *Photochemical & Photobiological Sciences*, **1**, 289-308. http://dx.doi.org/10.1039/b200178k

Scientific Research

Scientific Research Publishing (SCIRP) is one of the largest Open Access journal publishers. It is currently publishing more than 200 open access, online, peer-reviewed journals covering a wide range of academic disciplines. SCIRP serves the worldwide academic communities and contributes to the progress and application of science with its publication.

Other selected journals from SCIRP are listed as below. Submit your manuscript to us via either submit@scirp.org or Online Submission Portal.